Available online at www.sciencedirect.com
SCIENCE DIRECT
Engineering Structures 28 (2006) 1736–1744
ENGINEERING STRUCTURES
www.elsevier.com/locate/engstruct

Blast load assessment using hydrocodes

B. Luccioni[a,b,*], D. Ambrosini[a,c], R. Danesi[b]

[a] CONICET, Av. Rivadavia 1917, (1033 AAJ) Ciudad de Buenos Aires, Argentina
[b] Structures Institute, National University of Tucumán, Avenida Roca 1800, S.M. de Tucumán, Argentina
[c] Engineering Faculty, National University of Cuyo, Centro Universitario - Parque Gral. San Martín - (5500), Mendoza, Argentina

Received 25 April 2005; accepted 22 February 2006
Available online 4 May 2006

Abstract

The evaluation of pressures and impulses produced by blast loads with the aid of hydrocodes is studied in this paper. Numerical results are compared with those obtained with existing analytical expressions for different scaled distances and boundary conditions. In particular, the capacity of both methods to capture multiple reflections of the blast load is analyzed. The effects of mesh size on pressure and impulse distribution are also studied. Some interesting conclusions regarding the determination of the best mesh size for calculation of actual events are obtained. Finally, the analysis of blast load in the case of the AMIA (Israel–Argentina Mutual Association) building attack which occurred in Buenos Aires, Argentina in July 1994 is presented. A computational dynamic analysis was carried out over the congested urban environment that corresponds to the opposite rows of buildings of a block, in the same street. The results obtained for different positions of the explosive charge are presented and compared.

Keywords: Shock waves; Blast loads; Wave propagation; Wave reflection; Pressure distribution; Numerical analysis

1. Introduction

Due to different accidental or intentional events, related to important structures all over the world, explosive loads have received considerable attention in recent years. Unfortunately, the recent attack on the World Trade Center as well as many other attacks in the entire world show that the activity in connection with terrorism has increased and the present tendency suggests that it will be even larger in the future. This paper is concerned with the dynamic loading produced by the detonation of high explosive materials in urban environments, a situation likely to be expected in most terrorist attacks.

The design and construction of public buildings to provide life safety in the face of explosions is receiving renewed attention from structural engineers [1–3]. For many urban settings, the proximity to unregulated traffic brings the terrorist threat to or within the perimeter of the building. For these structures, blast protection has the modest goal of containing damage in the immediate vicinity of the explosion and the prevention of progressive collapse.

The assessment of blast loading effects on structures is required for the design of structures to withstand explosions. In this way, the first stage of the analysis is the accurate and reliable evaluation of the pressures and impulses acting on the structure.

On the other hand, when a blast attack has already occurred, a very important issue is the determination of the focus location of the explosion and the mass of the explosive used. A useful tool to achieve this objective is the evidence of the crater generated by the explosion. However, in many cases, the crater remains lost under parts of the destroyed structures and it is almost impossible to reconstruct its plan. Additionally, the mass of explosive obtained from crater dimensions has a significant spread. Some empirical expressions for crater dimensions can be found in the specialized literature [4,5] but according to Kinney and Graham [4], the results have a coefficient of variation of 30%. In all the cases mentioned above, the evaluation of pressures and impulses generated by the detonation through a computational analysis and the comparison with real damage registered in the urban

* Corresponding address: Calle Los Ceibos S/N, Country Las Yungas, Mendoza y Canal Yerba Buena, (4107) Yerba Buena, Tucumán, Argentina. Tel.: +54 381 4364087; fax: +54 381 4364087.
E-mail address: bluccioni@herrera.unt.edu.ar (B. Luccioni).

0141-0296/$ - see front matter © 2006 Elsevier Ltd. All rights reserved.
doi:10.1016/j.engstruct.2006.02.016

environment constitutes an attractive alternative for the determination of the location of the focus and the mass of the explosive charge.

Historically, the analysis of explosions either has predominantly involved simplified analytical methods [6,4,7] or has required the use of supercomputers for detailed numerical simulations. With the rapid development of computer hardware over the last decades, it has become possible to make detailed numerical simulations of explosive events in personal computers, significantly increasing the availability of these methods. On the other hand, new developments in integrated computer hydrocodes complete the tools necessary to carry out the numerical analysis successfully.

Important effects such as multiple blast wave reflections, the Mach effect, rarefactions, and the negative phase of the blast wave can be readily modeled in computational fluid dynamics (CFD) codes. Simplified analytical and semi-empirical techniques many times ignore such phenomena. Thus, modeling groups of buildings in congested city centers can be treated thoroughly only by the use of sophisticated CFD numerical calculations [8]. In this paper, the program AUTODYN-3D [9] is used for these purposes. AUTODYN-3D [9] is an integrated analysis program specifically designed for non-linear dynamics problems that uses finite difference, finite volume, and finite element techniques to solve a wide variety of non-linear problems in solid, fluid and gas dynamics. This type of program is sometimes referred to as a "hydrocode". The phenomena to be studied with such a program can be characterized as highly time dependent with both geometric non-linearities (e.g. large strains and deformations) and material non-linearities (e.g. plasticity, failure, strain-hardening and softening, multiphase equations of state). AUTODYN-3D [9] uses a coupled methodology to allow an optimum numerical solution for a given problem. With this approach, different domains of a physical problem, e.g. structures, fluids, gases, etc. can be modeled with different numerical techniques or processors most appropriate for that domain. Then these different domains are coupled together in space and time to provide an optimized solution. This capability makes this code [9] especially suitable for the study of interaction problems involving multiple systems of structures, fluids, and gases.

The various numerical processors available in AUTODYN-3D [9] generally use a coupled finite difference/finite volume approach. This scheme allows alternative numerical processors to be selectively used to model different components/regimes of a problem. Individual structured meshes operated on by these different numerical processors can be coupled together in space and time to efficiently compute structural, fluid, or gas dynamics problems including coupled problems (e.g. fluid–structure, gas–structure, structure–structure, etc.).

The distribution of pressures and impulses generated by a blast loading in a congested urban environment is described in this paper. The behavior of blast waves in this type of geometry is both difficult to predict and of great importance in assessing explosion effects on buildings and people.

It is well known that the accuracy of numerical results is strongly dependent on the mesh size used for the analysis. On the other side, the mesh size is also limited by the dimensions of the model and the computer capacity. One of the major features in the numerical simulation of blast wave propagation in large urban environments is the use of an adequate mesh size. The effect of mesh size for different boundary conditions is also addressed in this paper.

2. Generation of blast loading

The analysis of the blast wave propagation was performed in two stages. The first part of the analysis consists of the simulation of the explosion itself from the detonation instant and the second part consists of the propagation analysis of the blast wave generated by the explosion.

The use of symmetry conditions allows the spherical portion of the blast wave expansion to be represented by a spherical model. This is achieved by a one-dimensional (1D) mesh using spherical symmetry. The number of cells required to produce accurate solutions is greatly reduced when compared with a full 3D model. When the spherical blast wave begins to interact with obstacles, the flow becomes multi-dimensional. However, before this time, the 1D solution can be imposed or remapped onto a specific region of the multi-dimensional model. The 3D calculation can then proceed from that point.

In order to carry out a comparable analysis, the mass of the explosive is defined by TNT masses. The corresponding masses for other explosives can be obtained through the concept of TNT equivalence [10]. Different masses of explosive, from 1 kg to 500 kg of TNT, were used in the analysis.

AUTODYN [9] uses the differential equations governing unsteady material dynamic motion to express the local conservation of mass, momentum and energy. In order to obtain a complete solution, in addition to appropriate initial and boundary conditions, it is necessary to define a further relation between the flow variables. This can be found from a material model which relates stress to deformation and internal energy (or temperature). In most cases, the stress tensor may be separated into a uniform hydrostatic pressure (all three normal stresses equal) and a stress deviatoric tensor associated with the resistance of the material to shear distortion (as is the case for most materials in AUTODYN). Then the relation between the hydrostatic pressure, the local density (or specific volume) and local specific energy (or temperature) is known as an equation of state.

High explosives are chemical substances which, when subject to suitable stimuli, react chemically very rapidly releasing energy. In the hydrodynamic theory of detonation, this very rapid time interval is shrunk to zero and a detonation wave is assumed to be a discontinuity which propagates through the unreacted material instantaneously liberating energy and transforming the explosive into detonating products. Since the 1939–45 war, when there was naturally extensive study of the behavior of high explosives, there has been a continuous attempt to understand the detonation process and the performance of the detonation products, leading to considerable

improvements in the equation of state of the products. The most comprehensive form of equation of state developed over this period, the "Jones–Wilkins–Lee" (JWL) [9] equation of state is used in this paper,

$$p = C_1\left(1-\frac{\omega}{r_1 v}\right)\mathrm{e}^{-r_1 v} + C_2\left(1-\frac{\omega}{r_2 v}\right)\mathrm{e}^{-r_2 v} + \frac{\omega e}{v} \qquad (1)$$

where p is the hydrostatic pressure, $v = 1/\rho$ is the specific volume, ρ is the density and C_1, r_1, C_2, r_2 and ω (adiabatic constant) are constants and their values have been determined from dynamic experiments and are available in the literature for many common explosives.

It can be shown that at large expansion ratios the first and second terms on the right hand side of Eq. (1) become negligible and hence the behavior of the explosive tends towards that of an ideal gas. Therefore, at large expansion ratios, where the explosive has expanded by a factor of approximately 10 from its original volume, it is valid to switch the equation of state for a high explosive from JWL to ideal gas. In such a case the adiabatic exponent for the ideal gas, γ, is related to the adiabatic constant of the explosive, ω, by the relation $\gamma = \omega + 1$. The reference density for the explosive can then be modified and the material compression will be reset. Potential numerical difficulties are therefore avoided.

The initial detonation and expansion of the sphere of high explosive were modeled in a 1D, spherically symmetric model of 1 m radius with a JWL equation of state. Partway through the detonation process, and to avoid numerical errors, the material model for the high explosive was modified. The 1D expansion analysis continued until just prior to impingement of the blast wave on the rigid surface. At this time a 1D remap file was created and then imported into a three-dimensional model, allowing the reflection of the blast wave off the ground and walls to be modeled.

3. Blast wave propagation

The numerical analysis of the blast wave propagation for different boundary conditions and mesh sizes is presented in this section.

3.1. Free field explosion of spherical charges

When a condensed high explosive is detonated, a blast wave is formed. It is characterized by an abrupt pressure increase at the shock front, followed by a quasi-exponential decay back to ambient pressure and a negative phase in which the pressure is less than ambient pressure. The pressure–time history of a blast wave is often described by exponential functions such as Frielander's equation [7], which has the form

$$p(t) = p_o + p_s[1-(t-t_a)/T_s]\exp[-b(t-t_a)/T_s] \qquad (2)$$

where t is the time, p_o is the ambient pressure, p_s is the peak overpressure, T_s is the duration of the positive phase, t_a is the arrival time and b is a positive constant called the waveform parameter that depends on the peak overpressure.

The most widely used approach for blast wave scaling is Hopkinson's law [6] which establishes that similar explosive waves are produced at identical scaled distances when two different charges of the same explosive and with the same geometry are detonated in the same atmosphere. Thus, any distance R from an explosive charge W can be transformed into a characteristic scaled distance Z,

$$Z = R/W^{1/3} \qquad (3)$$

where W is the charge mass expressed in kilograms of TNT. The use of Z allows a compact and efficient representation of blast wave data for a wide range of situations.

There are many solutions for the wave front parameters from both numerical solution and experimental measurements [6,4,7]. The results are usually presented in graphics, tables or equations based on experimental or numerical results, such as the tables given by Kinney and Graham [4] or the following equations presented by Smith and Hetherington [7],

$$\begin{aligned} p_s &= 1407.2/Z + 554.0/Z^2 - 35.7/Z^3 + 0.625/Z^4 \text{ kPa} \\ &\quad 0.05 \le Z \le 0.3 \\ p_s &= 619.4/Z - 32.6/Z^2 + 213.2/Z^3 \text{ kPa} \\ &\quad 0.3 \le Z \le 1.0 \\ p_s &= 66.2/Z + 405.0/Z^2 - 328.8/Z^3 \text{ kPa} \\ &\quad 1.0 \le Z \le 10. \end{aligned} \qquad (4)$$

The accuracy of predictions and measurements in the near field is lower than in the far field, probably due to the complexity of blast phenomena [7].

In order to study the free propagation of blast waves in air, a 5 m by 5 m by 10 m volume of air was numerically modeled with four different mesh sizes: 50, 100, 250 and 500 mm, see Fig. 1. A three dimensional Euler FCT [9] (higher order Euler processor) subgrid was used for the air. The Euler-FCT processor has been optimized for gas dynamic problems and blast problems and it is much more efficient in comparison with a general purpose high resolution Euler processor. FCT stands for Flux Corrected Transport [11]. With FCT a high order solution is computed wherever this is possible in the flow field. The high order solution fluxes are corrected in the regions of shocks using a low order reference (transported and diffused) solution.

In order to simulate a free field explosion, flow out of air was allowed in all the model borders.

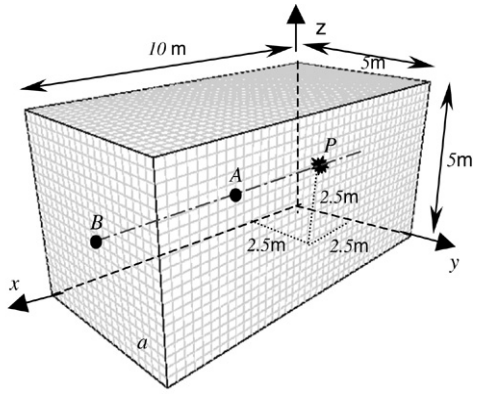

Fig. 1. Model for the study of blast wave free propagation.

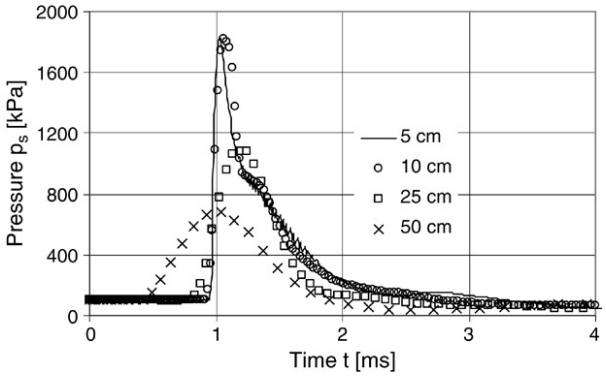

Fig. 2. Pressure–time history.

The results of the 1D analysis of explosive spherical charges ranging from 1 to 500 kg were mapped in the 3D air models at point P of coordinates $x = y = z = 2.5$ m that is indicated with a star in Fig. 1 and represents the location of the explosive charge.

Fig. 2 shows a pressure–time history curve obtained for point A of coordinates $x = 5.5$ m, $y = z = 2.5$ m, located at 3 m from a 100 kg of TNT explosive charge. It can be seen that the curves resemble that one described by Eq. (2), but there are important differences among the peak overpressures obtained for the different mesh sizes. It must be noted that, as the mesh is refined, the difference between the results for the different mesh sizes is reduced showing the convergence of numerical results.

Numerical results for the peak overpressure related to the ambient pressure p_s/p_o are compared with those obtained with empirical equations [6,7] in Fig. 3 for different scaled distances from the explosive charge. Numerical values are obtained for different points along the line defined by $y = z = 2.5$ m and indicated in Fig. 1. For high-scaled distances the results obtained with the finest mesh are much closer to empirical ones. As the scaled distance decreases, numerical results depart from empirical ones. Nevertheless, it may be noted that the accuracy of empirical relations in the near field is not guaranteed [7]. The difference with empirical values is more marked for coarser meshes that give lower values for the peak overpressure, but results tend to converge as the mesh is refined. The results corresponding to the meshes of 5 and 10 cm are almost coincident. It can be concluded that the mesh of 100 mm gives an accurate solution to the problem.

The comparison of maximum impulses is presented in Fig. 4. For high-scaled distances the impulses obtained with the finest mesh are much closer to the empirical ones. As the scaled distance decreases numerical results depart from empirical ones and the tendency is not as defined as in the case of pressures.

The comparison of maximum peak overpressures obtained with the finest mesh and experimental results [12,13] is presented in Fig. 5. A good agreement among numerical and experimental results is observed.

3.2. Reflected waves with normal incidence

When the blast waves encounter an infinite large wall on which they impinge at zero angle of incidence, they are normally reflected. All flow behind the wave is stopped and pressures are considerably greater than side-on.

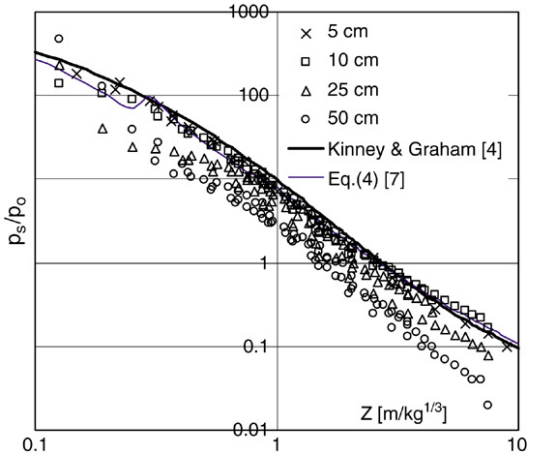

Fig. 3. Peak side-on overpressures as a function of scaled distance.

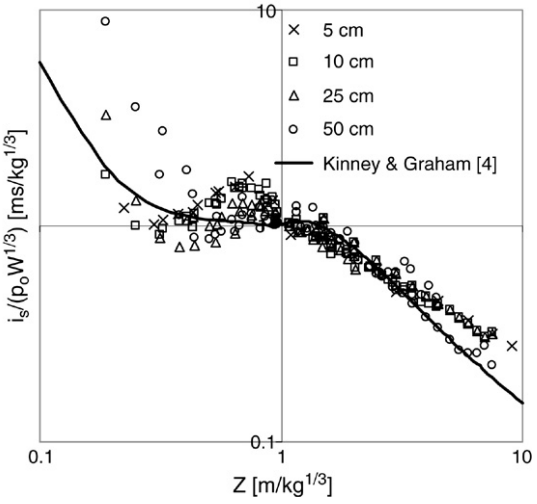

Fig. 4. Peak side-on impulses as a function of scaled distance.

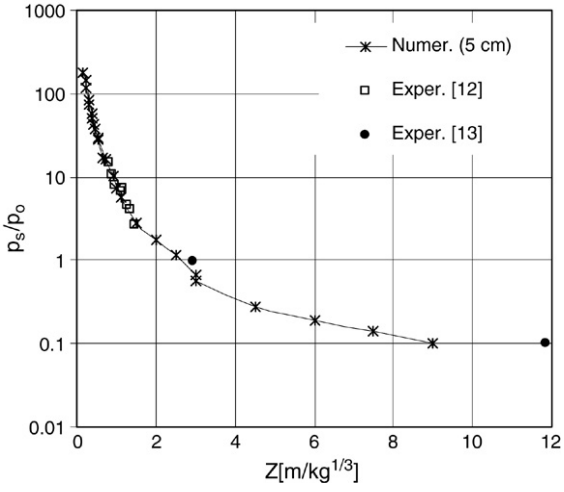

Fig. 5. Comparison of numerical and experimental values of peak side-on overpressures.

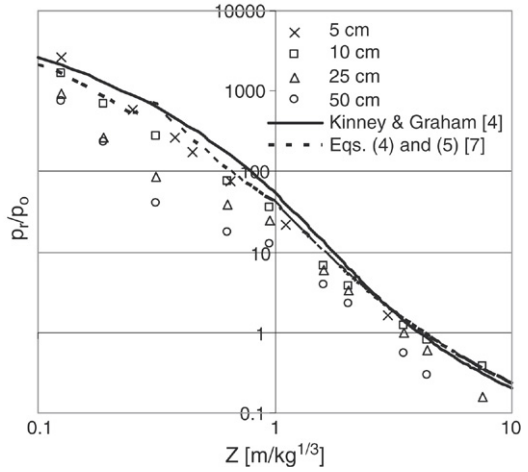

Fig. 6. Peak reflected overpressures as a function of scaled distance.

The peak reflected pressure p_r can be obtained from Rankine–Hugoniot relationships for an ideal gas and results [7],

$$p_r = 2p_s(7p_o + 4p_s)/(7p_o + p_s). \quad (5)$$

Lacking of more accurate prediction methods the reflected impulse can be estimated by assuming similarity between the time histories of side-on overpressures and normally reflected overpressure. This assumption gives [6],

$$i_r/i_s \approx p_r/p_s \quad (6)$$

where i_s is the peak side-on impulse and i_r is the peak reflected impulse.

In order to study the normal reflection of blast waves, the same numerical models presented in Fig. 1 were used, but this time an infinite rigid surface was defined on face a, normal to the wave direction. The comparison of peak reflected overpressures numerically obtained for point B ($x = 10$ m, $y = z = 2.5$ m), for different scaled distances from the explosive charge and different mesh sizes, and those obtained with Eq. (5) is presented in Fig. 6. Reflected impulses are compared in Fig. 7. The same conclusions as in the case of free propagation values can be stated but, in this case, the difference in impulse values for the different mesh sizes is lower.

3.3. Regular and Mach reflection

The most usual case of loading of large flat surfaces is represented by waves that strike at oblique incidence. For angles of incidence between 0° and 90°, either regular or Mach reflection occurs depending on incident angle and shock strength [6,7]. The evaluation of reflected pressures resulting from multiple reflections on surfaces with different incidence angles is very complicated and difficult to perform with empirical equations. In this case, the use of numerical methods is more appropriate.

In order to analyze the reflected pressures and impulses produced by this type of problem, the model presented in Fig. 8 was used. Faces a, b and c were considered to be infinitely rigid, while air flow out was allowed in the other faces. The dimensions of this model were chosen in order to get conclusions applicable to the example presented later in the paper.

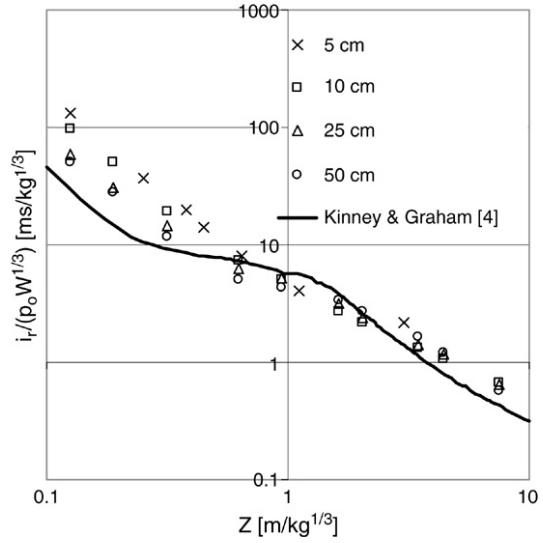

Fig. 7. Peak reflected impulses as a function of scaled distance.

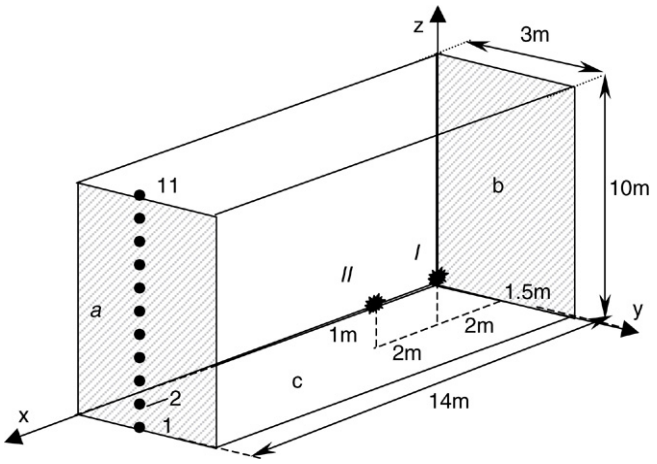

Fig. 8. Model for the study of blast wave propagation with oblique reflections.

Three different mesh sizes were used: 100, 250 and 500 mm. The finest mesh (50 mm) was not used because it requires too many cells and it has been proved that it gives results almost coincident with those of the 100 mm mesh. A spherical explosive charge of 300 kg of TNT with the location indicated as I in Fig. 8 was used for all the calculations.

Fig. 9 shows the pressure–time history obtained for point 2 (Fig. 8) with this model and that obtained for the same model but allowing air flow out in faces b and c. Both curves were obtained with the 100 mm mesh. The sub-estimation of the peak reflected pressure when reflection on faces b and c is neglected is clear in Fig. 9. The wave resulting from the reflection on face b is also clear in numerical results.

Figs. 10 and 11 show the values of peak reflected pressure and impulse respectively along a vertical line in face a (see Fig. 8) and the comparison with empirical values obtained only considering normal reflection on face a. It is clear that both pressure and impulse values are underestimated when the mesh gets coarser. But even for the 50 cm mesh, the values are

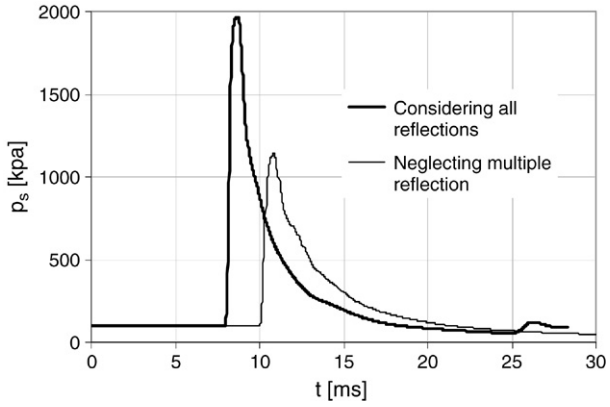

Fig. 9. Comparison of pressure–time histories for different reflecting conditions.

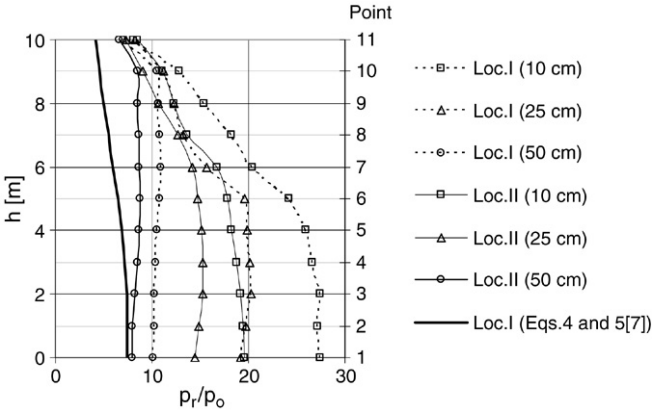

Fig. 10. Peak reflected overpressures along a vertical line.

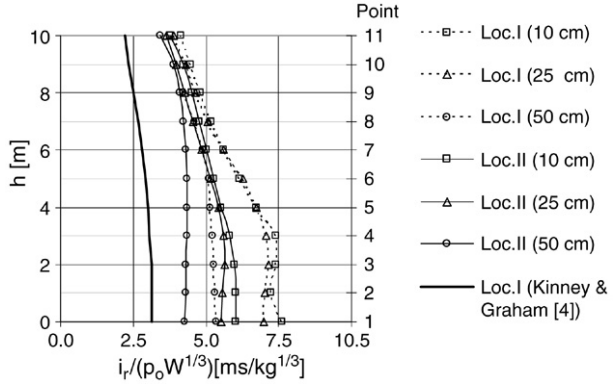

Fig. 11. Peak reflected impulses along a vertical line.

greater than those obtained empirically neglecting reflections on surfaces *b* and *c*.

Figs. 10 and 11 also show the comparison of pressure and impulse distributions along a vertical line when the explosive charge is moved to position II indicated in Fig. 8. It is clear that, although coarse meshes underestimate pressures and impulses, the effect of moving the explosive charge is qualitatively captured even by the coarsest mesh.

Fig. 12 shows the comparison of numerical values of peak overpressure along the line $y = 1.5$ m, $z = 1$ m in

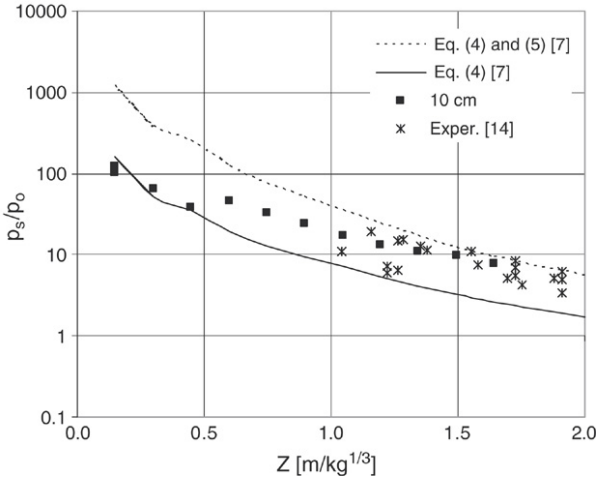

Fig. 12. Comparison of numerical and experimental values of peak overpressure.

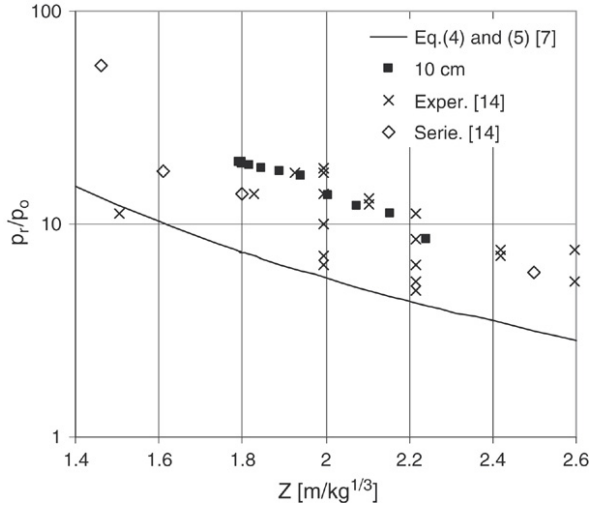

Fig. 13. Comparison of numerical and experimental values of peak reflected overpressure.

Fig. 8 and experimental values in Ref. [14]. Fig. 13 shows the values of peak reflected pressure along a vertical line in face *a* (see Fig. 8) and the comparison with experimental values in Refs. [14] and [15]. The tests included comprise a wide range of configurations which introduce the observed variability in experimental results.

Fig. 12 shows that side-on overpressures are underestimated by Eq. (4) because reflections on the ground are not considered and are overestimated by equation Eq. (5) describing normal reflections. Numerical results give a better approximation.

Fig. 13 shows that reflected pressures are also underestimated when they are evaluated with Eq. (5) for normal reflection neglecting other sources of reflection. Numerical results show a better agreement with experimental ones but they lie over the mean of experimental results. This fact can be attributed to the variability of test conditions and the differences between tests and the numerical model in model 8, particularly to the difference in reflecting properties between the ground and surface *b*.

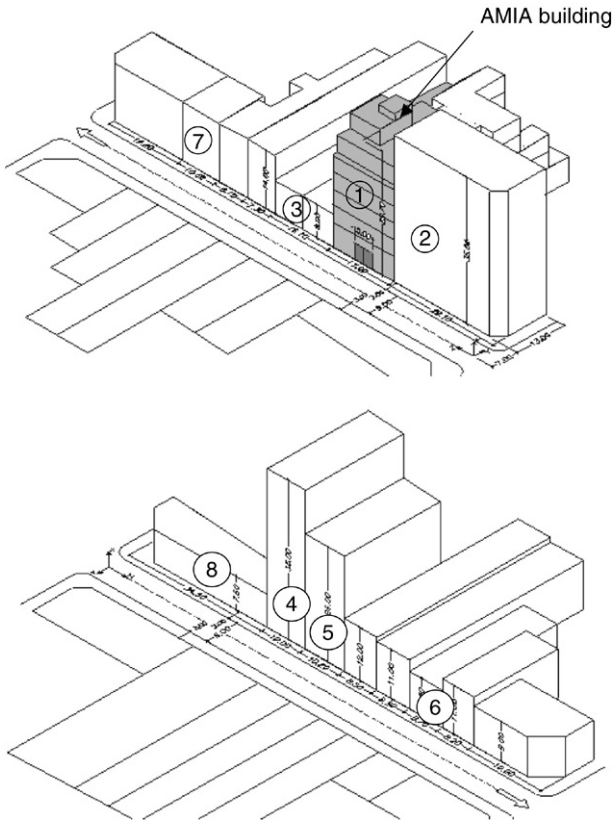

Fig. 14. Blast scenario.

4. Numerical simulation of an actual blast event in an urban environment

The evaluation of blast loads produced by the explosion that destroyed part of the AMIA (Israel–Argentina Mutual Association) building in the city of Buenos Aires in 1994 is presented in this section. The blast scenario is illustrated in Fig. 14 and corresponds to the two rows of buildings of a block, on the opposite sides of the same street.

Many alternatives of mass of explosive and locations were analyzed. 200, 300, 400 and 500 kg of TNT were used because they are in the medium range of terrorist attacks on buildings. The range of explosive masses used in terrorist attacks is discussed in some papers [1,2] and it is strongly dependent on how the explosive is supposed to have been transported. The trial locations were inferred from a visual inspection of photographs of damage and result in correspondence with the front of the target building. For sake of clarity, only the results correspondent to 300 kg of TNT in locations indicated as 1, 2 and 3 in the entrance of building 1 in Fig. 15 will be shown in this paper.

Due to the large dimensions of the problem analyzed and taking into account that the aim of this study was the comparison of the effects of different locations of the explosive on resulting blast loads on structures, a coarse mesh of 50 cm was used. Moreover, the model had to be split in two parts (Fig. 15) in order to make possible the computational analysis with a PC. Model 1 (380 000 cells) corresponds to the row of

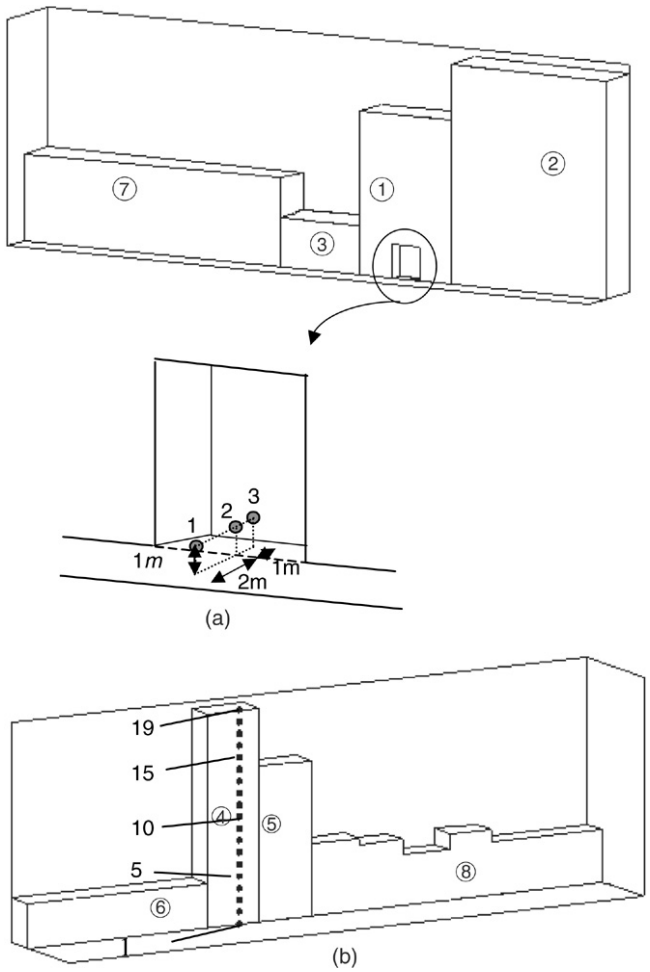

Fig. 15. Model for the simulation of an actual blast event (a) Part 1, (b) Part 2.

buildings where the target building was located and it extends up to the street axis. Model 2 (615 000 cells) corresponds to the row of building on the opposite side of the street. The numerical analysis presented in the previous section showed that, for the row of buildings closer to the explosive charge, the lost wave reflections on the facades of the buildings of the opposite side of the street are considerably out of phase with respect to the main shock. This fact is due to the relatively long distances involved. However, on the opposite side of the street (Model 2), the coupling between the waves generated by the main shock and that due to reflection on the target building is considerable. For this reason, the building facades that constitute the principal source of reflection were taken into account in Model 2. Particularly, the entrance hall of AMIA building had reflecting surfaces in its laterals but not at the back where there was an iron grating.

The buildings were defined as "unused" regions [9] and were considered to behave as rigid surfaces. Air flow out was allowed in the remaining boundaries of the model.

The dots in Fig. 15 represent the points where the pressure–time history was recorded during the numerical analysis.

The curves representing the time history of the reflected pressures and impulses for 300 kg TNT for location 1 are

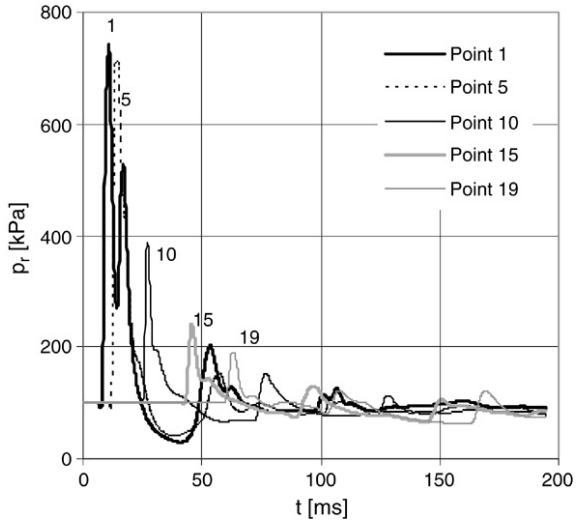

Fig. 16. Pressure–time histories for points 1, 5, 10, 15 and 19 (location 1).

presented in Fig. 16. These records correspond to the target points situated on a vertical line in the center of building 4 (see Fig. 15(b)). The results on the facade of this building were chosen for this analysis because they are more sensitive to the difference of blast load location than the other buildings.

Additionally, the distribution of peak reflected overpressures and impulses with height for building 4, for the different locations are presented in Fig. 17. The results obtained with empirical equations for normal reflection are also included in Fig. 17. When the explosive charge is moved away from the building analyzed the value of peak overpressure and impulse decreases until a certain limit when the pressure begins to increase due to the effects of reflections of the blast wave on the facades of the buildings on the opposite side of the street. It is clear that this effect cannot be achieved through the empirical expressions used.

The use of different analytical methods for the assessment of structures under blast loads can be found in the literature [6,4,7]. According to these methods, for the values of reflected pressure and impulse obtained, the level of damage is practically defined by the impulse value. With this consideration in view, the maximum reflected impulse contours for the three different locations analyzed are presented in Fig. 18. It can be seen that there is an appreciable difference in impulse values between locations 1 and 2 but not between locations 2 and 3 where the difference only appears for the buildings more distant from the explosion.

5. Conclusions

According to the results presented in the paper, it is clear that the use of empirical expressions is not enough for the accurate evaluation of incident pressure distributions and associated impulses in complex urban environments. Neglecting reflections and the 'Mach effect' of the blast wave could lead to important underestimation of the peak values in the far field. Moreover, empirical expressions are not applicable with confidence in the near field because of the complexity of the flow processes involved in forming the blast wave.

For these cases the detailed time history of side-on and reflected pressures and impulses can accurately be obtained with numerical methods such as hydrocodes. This type of analysis can reproduce not only free blast wave propagation but also normal and oblique reflection occurring on building facades.

The accuracy of numerical results is strongly dependent on the mesh size used for the analysis. A 10 cm mesh is accurate enough for the analysis of wave propagation in urban environments. Nevertheless it may be too expensive to model a complete block with this mesh size. Alternatively, a coarser mesh can be used in order to obtain qualitative results for the

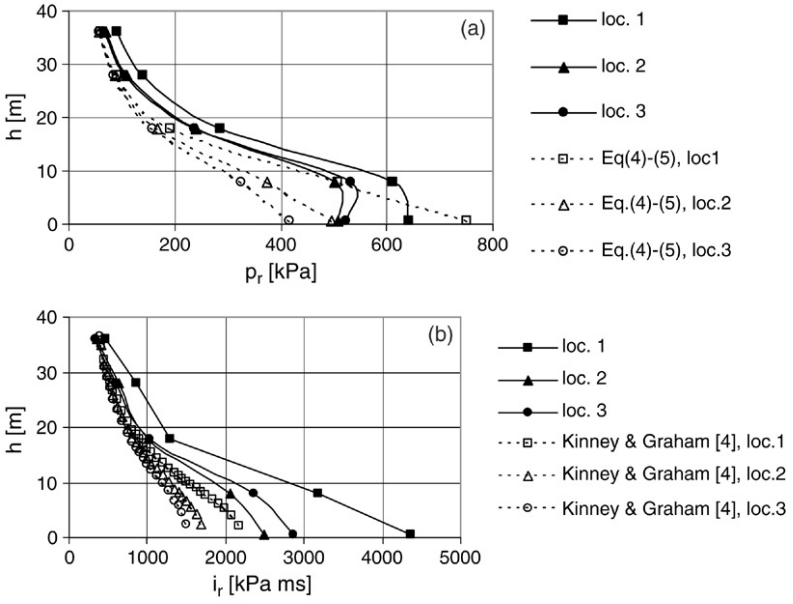

Fig. 17. Peak reflected values for different locations of the explosive charge. (a) Overpressures, (b) impulses.

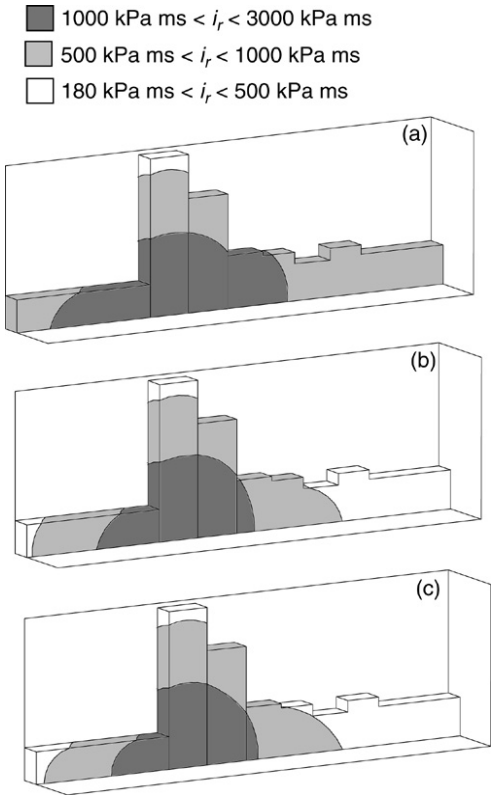

Fig. 18. Reflected impulse contours. (a) Location 1, (b) location 2, (c) location 3.

comparison of the loads produced by different hypothetical blast events. Even coarse meshes, up to 50 cm of side, give a good estimation of the effects of moving the location of the explosive charges.

The difference between numerical results for different mesh size increases with decreasing scaled distances. It may be marked that, even for the coarser mesh of 50 cm side, the results are more conservative than those obtained with empirical expressions neglecting multiple reflections that take part in actual situations.

Another important feature is that the differences obtained are lesser for the case of impulses than for the case of pressure. This conclusion is important taking into account that, for the range of scaled distances involved in actual urban environments, damage is practically defined by the value of the peak reflected impulse.

Acknowledgements

The authors wish to thank the collaboration of Engs. Sergio Gutiérrez and Abel Jacinto. The financial support of the CONICET, the National University of Tucumán and the Argentine Judiciary Board is gratefully acknowledged. Special acknowledgements are extended to Drs. Bence Gerber and Chris X. Quan for the technical support of AUTODYN and to Ms. Amelia Campos for the English revision.

References

[1] Elliot CL, Mays GC, Smith PD. The protection of buildings against terrorism and disorder. Proceedings of Institution of Civil Engineers: Structures & Buildings 1992;94:287–97.
[2] Millington G. Discussion of 'The protection of buildings against terrorism and disorder' by Elliot C.L., Mays G.C. and Smith P.D. Proceedings of Institution of Civil Engineers: Structures & Buildings 1994;104:343–50.
[3] Committee on feasibility of applying blast-mitigating technologies and design methodologies from military facilities to civilian buildings. Protecting buildings from bomb damage. Washington: National Academy Press; 1995.
[4] Kinney GF, Graham KJ. Explosive shocks in air. 2nd ed. Berlin: Springer Verlag; 1985.
[5] Ambrosini RD, Luccioni BM, Danesi RF, Riera JD, Rocha MM. Size of craters produced by explosive charges on or above the ground surface. Shock Waves 2002;12(1):69–78.
[6] Baker WE, Cox PA, Westine PS, Kulesz JJ, Strehlow RA. Explosion hazards and evaluation. Amsterdam: Elsevier; 1983.
[7] Smith PD, Hetherington JG. Blast and ballistic loading of structures. Great Britain: Butterworth-Heinemann Ltd; 1994.
[8] Smith PD, Rose TA. Blast loading and building robustness. Progress in Structural Engineering and Materials 2002;4(2):213–23.
[9] AUTODYN user's manual-revision 4.3. Century Dynamics Inc.; 2003.
[10] Formby SA, Wharton RK. Blast characteristics and TNT equivalence values for some commercial explosives detonated at ground level. Journal of Hazardous Materials 1996;50:183–98.
[11] Oran ES, Boris JP. Numerical simulation of reactive flow. Elsevier; 1987.
[12] Smith PD, Rose TA, Saotonglang E. Clearing of blast waves from building facades. Proceedings of Institution of Civil Engineers: Structures & Buildings 1999;134:193–9.
[13] MacPherson WN, Gander MJ, Barton JS, Jones JDC, Owen CL, Watson AJ et al. Blast-pressure measurement with a high-bandwidth fibre optic pressure sensor. Measurement Science and Technology 2000;11: 95–102.
[14] Bogosian D, Ferritto J, Shi Y. Uncertainty and conservatism in simplified blast models. In: 30th Explosives Safety Seminar; 2002.
[15] Lok TS, Xiao JR. Steel-fibre-reinforced concrete panels exposed to air blast loading. Proceedings of the Institution of Civil Engineers: Structures & Buildings 1999;134:319–31.